Horizon | Journal of Humanity and Artificial Intelligence

Volume 3, Issue 3 | 2024 *https://univerpubl.com/index.php/horizon*
ISSN: 2835-3064

Article

Mechanosynthesis, Characterization, and Antimicrobial Evaluation of Cadmium(II), Nickel(II), Iron(III), and Chromium(III) Chelates Formed with Paracetamol and Aspirin

J. Ibrahim[1]*, A. Sumaila[2]

1.2 Department of Chemistry, Faculty of Science, Confluence University of Science and Technology, Osara. Km 19 Okene - Lokoja Road, P.M.B.1040 Osara, Kogi State, Nigeria
* Correspondence: ibrahimj@custech.edu.ng

Abstract: This study describes the mechanochemical synthesis of cadmium (Cd(II)), nickel (Ni(II)), and chromium (Cr(III)) as well as iron (Fe(III)) complexes with aspirin and paracetamol, achieved through simple grinding of their metal chlorides without the use of solvents. Additionally, these complexes were prepared using traditional solution-based methods for comparison. Both mechanochemical and conventional products were characterized by examining their solubility, melting points, conductivity, magnetic moments, and infrared (IR) spectra. The IR and analytical data indicated that the complexes formed were identical regardless of the synthesis method. Job's method analysis showed a 1:2 metal-to-ligand ratio for both aspirin and paracetamol complexes. High molar conductance values, ranging from 109.42 to 207.61 $\Omega^{-1}cm^2mol^{-1}$ for aspirin complexes and 77.32 to 100.22 $\Omega^{-1}cm^2mol^{-1}$ for paracetamol complexes, suggest their electrolytic nature in dimethylsulfoxide (DMSO). The complexes were soluble in dimethylformamide (DMF) and DMSO, with paracetamol complexes also dissolving in acetone, methanol, and diethylether (DEE), and aspirin complexes being soluble in methanol, DMF, and DMSO. Except for the Cr(III) complex, all aspirin complexes were insoluble in water. Magnetic moment values confirmed that all synthesized complexes were paramagnetic, except for the diamagnetic cadmium complexes. The complexes displayed higher thermal stability, decomposing between 163.7-198.3 °C, compared to their respective ligands which decomposed at 170 °C for paracetamol and 137 °C for aspirin. The antimicrobial activity of the ligands and their complexes was tested against two bacterial strains, *Escherichia coli* and *Staphylococcus aureus*, and two fungal strains, *Mucus species* and *Candida species*. The ligands exhibited limited activity against most organisms, whereas most complexes showed activity at all test concentrations, with paracetamol complexes being effective only at higher concentrations.

Keywords: Mechanosynthesis, Characterization, and Anti-Microbial Screening; Cd(II), Ni(II), Fe(III), and Cr(III) chelates; Paracetamol and Aspirin

Citation: Ibrahim, J., & Sumaila, A. Mechanosynthesis, Characterization, and Antimicrobial Evaluation of Cadmium(II), Nickel(II), Iron(III), and Chromium(III) Chelates Formed with Paracetamol and Aspirin. Horizon: Journal of Humanity and Artificial Intelligence 2024, 3(3), 80-105.

Received: 22nd July 2024
Revised: 29th July 2024
Accepted: 5th August 2024
Published: 12th August 2024

1. Introduction

The increasing scarcity of energy and material resources, along with the growing concern over industrial pollution, has made the development of cleaner and more efficient synthetic methods essential for modern research (Mottillo et al., 2013). For years, chemists worldwide have been exploring the reactivity of matter to design and create new chemicals for various applications with significant economic impacts, particularly in the health and chemical industries (Cisneros-de et al., 2016).

Recent studies have demonstrated that mechanical force can effectively drive chemical transformations in the solid state (Prochowicz et al., 2016). Mechanochemical reactions, which occur without solvents, are environmentally friendly due to their low energy consumption, reduced reaction times, minimized reagent use, and elimination of solvent

waste (James et al., 2012; Cisneros-de et al., 2016). The development of new materials for solid-state science and technology relies on innovative synthetic methods, highlighting the need to explore solvent-free synthesis (Kurawa, 2008). Recent research has shown that various coordination compounds can be synthesized without the use of solutions (James et al., 2012; Kurawa and Yammama, 2014).

Mechanochemical reactions have been extensively studied by Prof. Janusz Lewiński's team at the Institute of Physical Chemistry of the Polish Academy of Sciences (IPC PAS) and the Faculty of Chemistry at Warsaw University of Technology. Their recent publication describes a simple and effective method for synthesizing perovskites, which are advanced photovoltaic materials with complex crystal structures. Prof. Lewiński notes that mechanochemistry enables the synthesis of hybrid inorganic-organic functional materials with significant potential for the energy sector, including high-quality perovskites for efficient solar cells (Prochowi et al., 2016). Mechanochemistry involves chemical reactions triggered by mechanical energy, where reactants are ground between balls or between a ball and a wall, absorbing energy from the collisions to facilitate the reaction (Dennehy and Collins, 2016; Mochales et al., 2004).

Mechanochemistry involves reactions, typically of solids, driven by mechanical energy, such as grinding in ball mills. This method is gaining attention because it can rapidly and effectively promote reactions between solids with little or no solvent use. Traditionally, it was a secondary approach to chemical synthesis, with solution-based methods being more common. However, mechanochemistry has the potential to become a mainstream technique for two main reasons. First, it has proven effective and advantageous for a growing range of syntheses. Second, reliance on solvents is increasingly seen as unsustainable due to the waste of fossil-derived materials, environmental issues, hazards, and the energy demands of solvent production, purification, and recycling (Stuart et al., 2012).

Solid-state synthesis in molecular coordination chemistry has been established for a long time but remains underutilized (Adams et al., 2010). Recent interest in solid-state synthesis has grown because these reactions can be more convenient, cost-effective, and environmentally friendly compared to solvent-based methods. They also enhance safety, simplify work-up, and provide faster access to complexes that are difficult or time-consuming to synthesize using other methods. For example, the assembly of a hexa-palladium bowl-shaped cluster was achieved in just ten minutes at room temperature by grinding [Pd(NO_3)$_2$en] with a tripodal ligand, whereas a similar reaction with platinum took over four weeks at 100 ºC in D_2O.

Metal complexes are now central to drug design due to the success of metallodrugs like Auranofin, Flamazine, and Cisplatin. This success has expanded the database of chemotherapeutic agents that are less toxic and have improved anticancer, antioxidant, and antimicrobial properties. Consequently, metal complexes are considered potential lead compounds for developing new drugs to combat toxicity and resistance (Chandrathilaka et al., 2013).

Research has shown that grinding protonated ligands [H_2LCl] (where L represents imidazole or pyrazole) with metal dichlorides (MCl_2, where M is Co, Cu, or Zn) in the solid state leads to the formation of hydrogen-bonded metal salts [H2im]2[MCl_4] and [H2pz]2[MCl_4] for Co and Zn. Additionally, similar salts with Palladium and Platinum can be prepared using solid-state methods to produce [H2im]2[MCl_4] (where M is Pd or Pt) (Kurawa et al., 2008).

Metal ion complexation is a fundamental and diverse reaction class, characterized by varying degrees of lability and applications ranging from small-scale uses like radiopharmaceuticals to large-scale processes like metal extraction. Traditionally developed as solution-state chemistry, metal complexation is increasingly being achieved through solvent-free grinding and liquid-assisted grinding (LAG), as indicated by a growing body of literature (Stuart et al., 2013).

A recent study highlighted that metal-organic frameworks (MOFs) can be synthesized via solid-state grinding, yielding structures identical to those produced hydrothermally. For instance, a report in CrystEngComm demonstrated that the microporous MOF [Cu(INA)$_2$] (INA representing isonicotinic acid) can be formed by grinding precise amounts of starting materials in a ball mill. This environmentally friendly approach, conducted at room temperature, avoids the risk of ligand decomposition and aligns with the increasing emphasis on sustainable chemistry (Marshall, 2015).

With increasing emphasis on environmentally friendly and atom-efficient processes, using green solvents like water or opting for solventless methods is becoming a favored approach in organic chemistry. In recent years, solvent-free synthesis of heterocycles has emerged as a powerful technique, producing less toxic waste and reducing environmental impact. Mechanical forces such as grinding or milling have been extensively employed in solventless organic syntheses. Mechanochemical solid-state reactions, including dry co-grinding, have been explored for various chemical transformations, such as the creation of amides, thioureas, metallodrugs, coupling reactions, and asymmetric reactions. Numerous reviews highlight the history and successes of mechanochemistry (Katritzky, 2014).

Mechanochemically driven solid-state processes have gained significant attention due to their potential technological applications, particularly in developing environmentally friendly and cost-effective dry processes. The mechanochemical synthesis of nanocrystalline materials is a rapidly growing field in solid-state science, encompassing areas like alloys, nanostructured materials, and nanomagnets (Olmos et al., 2008).

Many people have used aspirin, but few know that its related compound from willow bark has been used for pain relief and fever treatment for centuries. Ancient Asian records document its use as far back as 2400 years ago (Lewis, 2003).

2. Materials and Methods

All reagents and chemicals used were of analytical grade and were used without further purification. The active pharmaceutical ingredients, aspirin and paracetamol powders, were sourced from Dana Pharmaceutical Company in Minna, Nigeria. The metal salts utilized included Cadmium(II) chloride, Nickel(II) chloride, Iron(III) chloride, and Chromium(III) chloride.

All glassware was thoroughly washed with detergent, rinsed with distilled water, and dried in an oven at 110 °C. Weighings were performed using a Mettler Toledo balance, model B154. Infrared spectra of the ligands and complexes were recorded with a Shimadzu FTIR 8400S Fourier Transform Infrared Spectrophotometer, covering band ranges from 380 to 4000 cm^{-1}. UV-absorbance measurements were taken with a Jenway 6305 UV-Visible Spectrophotometer, and molar conductance was measured using a Jenway 4010 conductivity meter in DMSO. Magnetic susceptibility of the complexes was measured using a MK 1 Shanwood magnetic susceptibility balance. Decomposition and melting temperatures were recorded with a Gallen Kamp melting apparatus. Bacteria and fungi isolates, including *Escherichia coli, Klebsiella pneumoniae*, *Staphylococcus aureus*, *Aspergillus fumigatus*, and a *Mucor species*, were obtained and identified at the Department of Microbiology, Bayero University Kano.

Synthesis of the Complexes

The complexes were synthesized using two methods: a mechanochemical approach (grinding without solvent using a mortar and pestle for 5-10 minutes) and a conventional solution-based method (refluxing with ethanol for 3-4 hours) as a reference.

Mechanosynthesis of Cadmium(II) Aspirin Complex:

A mixture of 1.833 g (0.01 mol) of $CdCl_2$ and 3.603 g (0.02 mol) of aspirin was ground using an agate mortar and pestle until a fine creamy-white powder was formed, which emitted a choking odor. The product was then dried in a desiccator to yield the complex (Kurawa and Yammama, 2014).

Solution-Based Synthesis of Cadmium(II) Aspirin Complex:

The complex was prepared by mixing an aqueous solution of $CdCl_2$ (0.01 mol, 1.833 g) in 10 ml of distilled water with an ethanolic solution of aspirin (0.02 mol, 3.603 g) in 20 ml. This mixture was refluxed with constant stirring for 4 hours and then left for 24 hours to complete the complexation. The precipitated complex was filtered, washed with cold ethanol, and dried in a desiccator (Lawal and Obaleye, 2007).

Mechanosynthesis of Nickel(II) Aspirin Complex:

A mixture of 2.3769 g (0.01 mol) of $NiCl_2{\cdot}6H_2O$ and 3.603 g (0.02 mol) of aspirin was ground using an agate pestle and mortar until a lemon-green powder was formed, emitting a choking odor. The product was then dried in a desiccator to yield the complex (Kurawa and Yammama, 2014).

Solution-Based Synthesis of Nickel(II) Aspirin Complex:

The complex was prepared by mixing an aqueous solution of $NiCl_2{\cdot}6H_2O$ (0.01 mol, 2.3769 g) in 10 ml of water with an ethanolic solution of aspirin (0.02 mol, 3.603 g) in 20 ml. This mixture was refluxed with constant stirring for 4 hours and then left for 24 hours. The resulting crystalline solid was filtered, washed with cold ethanol, and dried for 48 hours in a desiccator (Lawal and Obaleye, 2007).

Mechanosynthesis of Iron(III) Aspirin Complex:

A mixture of 2.70 g (0.01 mol) of $FeCl_3{\cdot}6H_2O$ and 3.603 g (0.02 mol) of aspirin was ground using an agate mortar and pestle until a black paste was formed. This paste was then dried in a desiccator for 48 hours (Kurawa and Yammama, 2014).

Solution-Based Synthesis of Iron(III) Aspirin Complex:

An aqueous solution of $FeCl_3{\cdot}6H_2O$ (2.705 g, 0.01 mol) in 10 ml of water was mixed with an ethanolic solution of aspirin (3.603 g, 0.02 mol) in 20 ml. The mixture was refluxed with constant stirring for three hours, then stored in a covered beaker at room temperature. After 24 hours, a solid precipitate formed, which was filtered, washed with cold ethanol, and dried in a desiccator for 48 hours (Lawal and Obaleye, 2007).

Mechanosynthesis of Chromium(III) Aspirin Complex:

A mixture of 1.23 g (0.01 mol) of $CrCl_3$ and 3.603 g (0.02 mol) of aspirin was ground using an agate mortar and pestle until a whitish-purple powder was obtained. This product was then stored in a desiccator for 24 hours (Kurawa and Yammama, 2014).

Solution-Based Synthesis of Chromium(III) Aspirin Complex:

An aqueous solution of $CrCl_3$ (1.23 g, 0.01 mol) in 10 ml of water was added to an ethanolic solution of aspirin (3.603 g, 0.02 mol) in 20 ml. The mixture was refluxed with constant stirring for three hours, then stored at room temperature for 24 hours. The whitish-purple crystalline complex was separated by filtration, washed with cold ethanol, and dried in a desiccator (Lawal and Obaleye, 2007).

Mechanosynthesis of Cadmium(II) Paracetamol Complex:

A mixture of 1.833 g (0.01 mol) of $CdCl_2$ and 3.023 g (0.02 mol) of paracetamol was ground using an agate mortar and pestle until a fine creamy powder was obtained. This product was then dried in a desiccator to form the complex (Kurawa and Yammama, 2014).

Solution-Based Synthesis of Cadmium(II) Paracetamol Complex:

An aqueous solution of $CdCl_2$ (1.833 g, 0.01 mol) in 10 ml of water was mixed with an ethanolic solution of paracetamol (3.023 g, 0.02 mol) in 25 ml. The mixture was refluxed with constant stirring for three hours and then left for 24 hours. The precipitated complex was filtered, washed with cold ethanol, and dried in a desiccator (Lawal and Obaleye, 2007).

Mechanosynthesis of Nickel(II) Paracetamol Complex:

A mixture of 2.3769 g (0.01 mol) of $NiCl_2 \cdot 6H_2O$ and 3.023 g (0.02 mol) of paracetamol was ground using an agate mortar and pestle until a whitish-blue powder was obtained. This product was then dried in a desiccator to form the complex (Kurawa and Yammama, 2014).

Solution-Based Synthesis of Nickel(II) Paracetamol Complex:

An aqueous solution of $NiCl_2 \cdot 6H_2O$ (2.376 g, 0.01 mol) in 10 ml of water was added to an ethanolic solution of paracetamol (3.023 g, 0.02 mol) in 25 ml. The mixture was refluxed with constant stirring for three hours and then left for 24 hours. The precipitated complex was filtered, washed with cold ethanol, and dried in a desiccator (Lawal and Obaleye, 2007).

Mechanochemical Synthesis of Iron(III) Paracetamol Complex:

A mixture of 2.705 g (0.01 mol) of $FeCl_3 \cdot 6H_2O$ and 3.023 g (0.02 mol) of paracetamol was ground using an agate mortar and pestle until a moist paste was obtained. This product was then dried in a desiccator (Kurawa and Yammama, 2014).

Solution-Based Synthesis of Iron(III) Paracetamol Complex:

An aqueous solution of $FeCl_3 \cdot 6H_2O$ (2.705 g, 0.01 mol) in 10 ml of water was combined with an ethanolic solution of paracetamol (3.023 g, 0.02 mol) in 20 ml. This mixture was refluxed with constant stirring for three hours and then left to stand for 24 hours. The precipitated complex was filtered, washed with cold ethanol, and dried in a desiccator (Lawal and Obaleye, 2007).

Mechanochemical Synthesis of Chromium(III) Paracetamol Complex:

A mixture of 1.23 g (0.01 mol) of $CrCl_3$ and 3.023 g (0.02 mol) of paracetamol was ground using an agate mortar and pestle until a moist dark or dirty white powder was obtained. This product was then dried in a desiccator (Kurawa and Yammama, 2014).

Solution-Based Synthesis of Chromium(III) Paracetamol Complex:

An aqueous solution of $CrCl_3$ (1.23 g, 0.01 mol) in 10 ml of water was added to an ethanolic solution of paracetamol (3.023 g, 0.02 mol) in 20 ml. The mixture was refluxed with constant stirring for three hours and then left to stand for 24 hours. The precipitated complex was filtered, washed with cold ethanol, and dried in a desiccator (Lawal and Obaleye, 2007).

Solubility Test:

The solubility of the Schiff base and the metal complexes was tested in various solvents including water, ethanol, methanol, dimethylformamide, acetone, dimethylsulfoxide, diethyl ether, chloroform, nitrobenzene, formaldehyde, and petroleum ether. The results are displayed in a table.

Molar Conductance Measurement of the Ligands and Their Complexes:

Molar conductance was measured by dissolving 0.2 g of each sample in 10 ml of DMSO in a test tube. An electrode was inserted to record the conductance values, and the molar conductance of each metal complex was evaluated. The results are presented in table 4.1.6.

Magnetic Susceptibility Measurement:

To measure magnetic susceptibility, the metal complex is inserted into a balance's capillary tube up to a designated mark. The recorded reading is then used in a formula to calculate the magnetic susceptibility value, Xg.

$$X_g = \frac{C \times L\ (R - R_\circ)}{10^9 M}$$

Where:

- C = 1, the proportionality constant
- L = the length of the sample in centimeters

- R = the reading obtained with the sample in the tube
- Ro = the reading obtained with the empty tube
- M = (Ws – Wo), the mass of the sample in grams, where Ws is the weight of the sample plus tube and Wo is the weight of the empty tube to determine the effective magnetic moment:
- Calculate Xm by multiplying the magnetic susceptibility (Xg) by the molar mass (molar magnetic moment).
- Compute the effective magnetic moment (μeff) using the formula: μeff = 2.828 $(Xm \times T)^{1/2}$, where T is the absolute temperature.

Melting Point and Decomposition Temperature Analysis

To determine the melting points of the ligands and the decomposition temperatures of their complexes, a small amount of each sample was placed into a capillary tube, which was then inserted into a Gallemkamp melting point apparatus. The temperatures at which the ligands melted and the complexes decomposed were recorded and are summarized in Table 4.1.2.

Determination of Metal-to-Ligand Ratio Using Job's Method

Job's method of continuous variation was employed to ascertain the metal-to-ligand ratio in the complex compounds (Angelici, 1971). Solutions of ligands and metal salts, each with a concentration of 3 millimolar, were prepared. Various metal-to-ligand ratios were tested, including 0:16, 1:15, 3:13, 5:11, 7:9, 9:7, 11:5, 13:3, and 15:1, maintaining a total solution volume of 16 ml for each mixture. The mole fraction of the ligand was calculated for each ratio. Metal salt solutions were scanned as blanks to determine the wavelength of maximum absorption (λmax) for each metal ion. Absorbance measurements were taken at λmax, and the number of ligands coordinated to the metal was determined by plotting absorbance against the ligand's mole fraction:

$$n = X_i/(1-X_i)$$

Where n represents the count of ligands coordinated, and xi denotes the mole fraction observed at peak absorbance.

Gravimetric Analysis for Metal Estimation in Complexes:

To estimate metals in complexes, 0.2 g of each complex is dissolved in 25 cm^3 of distilled water with 5 cm^3 of concentrated nitric acid, stirred vigorously, and then heated almost to dryness. The cooled mixture is filtered to obtain a solution containing metal ions (Vogel, 1989; Adamu, 2009).

For nickel(II) complexes, the filtrate is diluted with 97 cm^3 of distilled water, heated to 70–80°C, and treated with a slight excess of 1% dimethylglyoxime (DMG) in alcohol and dilute ammonia solution. After cooling, the precipitate is filtered, dried at 110°C, and weighed as $[Ni(C_4H_7O_2N_2)_2]$ (Vogel, 1989).

For iron(III) complexes, the filtrate is diluted to 100 cm^3 with distilled water, then treated with aqueous ammonia until precipitation begins. The mixture is heated, cooled, filtered, washed with 75 cm^3 of 1% ammonium nitrate, and dried at 110 °C before weighing as Fe_2O_3 (Vogel, 1989).

For Cadmium (Cd(II) Complexes, A 150 cm^3 solution of the cadmium(II) complex is prepared and boiled. After removing the heat source, a 3.3 % quinaldic acid solution is added dropwise with stirring until slightly excess. Dilute ammonia is then added dropwise. Upon cooling, a curdy white precipitate forms, which is filtered, washed with cold water, dried at 125 °C to constant weight, and weighed as $Cd(C_{10}H_6O_2)_2$ (Vogel, 1989).

For Chromium (Cr(III) Complexes, The Cr(III) complex filtrate is diluted to 100 cm^3 with distilled water. Sodium hydroxide is added until precipitation starts. An acetate buffer (10 cm^3 of 6 M acetic acid and 0.6 M sodium acetate) is followed by 10 cm^3 each of lead nitrate (3.5 g/100 cm^3) and potassium bromate (2.0 g/100 cm^3) solutions. The mixture

is heated to 90-95°C, then cooled, filtered, washed with 0.1% nitric acid, dried at 120°C, and weighed as $PbCrO_4$ (Vogel, 1989).

For Water Hydration In The Complex Compounds, For each complex, 0.2 g was heated at 110 °C until a constant weight was achieved. The water content in the complex was then calculated using the provided formula, with results detailed in Table 4.2.4.

$$\%\ \text{of water loss} = \frac{\text{lost in weight}}{\text{weight of the complex taken } (0.2\text{g})} \times \frac{100\%}{1}$$

(Aliyu and Abdullahi, 2009).

Antimicrobial Activity Test

The ligands and their corresponding metal complexes were tested for antibacterial activity against Escherichia coli and Staphylococcus aureus, as well as antifungal activity against Candida species and Mucor species.

Antibacterial Activity Test

Using the dilution method described by Yusha'u and Salisu (2011), various test concentrations were prepared. A stock solution was made by dissolving 0.06 g of the ligands or metal complexes in 1 cm^3 of DMSO, resulting in a concentration of 60 μg per cm^3. From this stock solution, a 30 μg concentration was prepared by mixing 0.5 cm^3 of the stock solution with 0.5 cm^3 of DMSO. Further dilution to 15 μg was achieved by taking 0.5 cm^3 of the 30 μg solution and adding 0.5 cm^3 of DMSO.

Paper discs were soaked in these various concentrations and used to inoculate culture plates containing nutrient agar. The plates were incubated at 37 °C for 24 hours. The antibacterial activity was assessed by measuring the diameter of the inhibition zones (Yusha'u and Salisu, 2011).

Antifungal Activity Test

The antifungal activity was evaluated using the dilution method outlined by Yusha'u and Salisu (2011). To prepare the test concentrations, 0.06 g of either the ligand or its metal complexes were dissolved in 1 cm^3 of DMSO, resulting in a stock solution with a concentration of 60 μg per cm^3. A 30 μg solution was created by mixing 0.5 cm^3 of the stock solution with 0.5 cm^3 of DMSO. Similarly, a 15 μg solution was prepared by diluting 0.5 cm^3 of the 30 μg solution with an additional 0.5 cm^3 of DMSO. These different concentrations were used to impregnate 50 paper discs, which were then used to inoculate culture plates. The plates, containing sabouraud dextrose agar, were incubated at room temperature for 48 hours. The antifungal activity of the ligands and their complexes was assessed using the paper disc technique, with the inhibition zones measured after 72 hours, as per Hassan et al. (2006).

3. Results

The findings from the analysis of the ligand and its metal complexes are detailed below:

Table 4.1.1. Physical Characteristics of Paracetamol and Its Metal Complexes Produced Using Both Methods

Compound	Method	% Yield	Colour	Melting Temperature (°C)	Decomposition Temperature (°C)
Paracetamol	-	-	White	170	-
$[Cd(Par)_2(H_2O)_2] \cdot 2H_2O$	Mech.	78.11	Creamy-white	-	191.4
$[Cd(Par)_2(H_2O)_2] \cdot 2H_2O$	Solution	60.87	Creamy-white	-	189.6
$[Ni(Par)_2(H_2O)_2] \cdot 2H_2O$	Mech.	87.42	Pinkish-white	-	192.9
$[Ni(Par)_2(H_2O)_2] \cdot 2H_2O$	Solution	63.20	Pinkish-white	-	193.7
$[Fe(Par)_2(H_2O)_2]Cl.2H_2O$	Mech.	82.53	Black	-	198.3
$[Fe(Par)_2(H_2O)_2]Cl.2H_2O$	Solution	61.14	Black	-	196.6
$[Cr(Par)_2(H_2O)_2]Cl.2H_2O$	Mech.	86.74	Whitish-Blue	-	187.6
$[Cr(Par)_2(H_2O)_2]Cl.2H_2O$	Solution	66.84	Whitish-Blue	-	187.8

Table 4.1.2. Physical Characteristics of Aspirin and its Metal Complexes Synthesized by both Methods

Compound	Method	% Yield	Colour	Melting Temperature (°C)	Decomposition Temperature (°C)
Aspirin	-	-	White	137	-
$[Cd(Asp)_2(H_2O)_2] \cdot 2H_2O$	Mech.	91.00	White	-	172.4
$[Cd(Asp)_2(H_2O)_2] \cdot 2H_2O$	Solution	69.21	White	-	169.7
$[Ni(Asp)_2(H_2O)_2] \cdot 2H_2O$	Mech.	80.53	Pale-green	-	178.3
$[Ni(Asp)_2(H_2O)_2] \cdot 2H_2O$	Solution	53.81	Pale-green	-	167.8
$[Fe(Asp)_2(H_2O)_2]Cl.2H_2O$	Mech.	79.10	Black	-	163.7

$[Fe(Asp)_2(H_2O)_2]Cl.2H_2O$	Solution	58.33	Black	-	164.5
$[Cr(Asp)_2(H_2O)_2]Cl.2H_2O$	Mech.	79.12	Pale-blue	-	181.3
$[Cr(Asp)_2(H_2O)_2]Cl.2H_2O$	Solution	58.34	Pale-blue	-	178.6

Table 4.1.3. Solubility of Paracetamol and Its Metal Complexes Prepared by Both Methods

Ligand /Compound	Method	Distilled Water	Ethanol	Methanol	Acetone	Chloroform	DEE	Petroleum Ether	DMF	DMSO	Nitro-Benzene
Paracetamol	-	SS	S	S	SS	SS	SS	SS	S	S	IS
$[Cd(Par)_2(H_2O)_2].\ 2H_2O$	Mech.	IS	IS	SS	S	IS	S	IS	S	S	IS
$[Cd(Par)_2(H_2O)_2].\ 2H_2O$	Soln.-based	IS	IS	SS	S	IS	S	IS	S	S	IS
$[Ni(Par)_2(H_2O)_2].\ 2H_2O$	Mech.	IS	IS	S	S	IS	S	IS	S	S	IS
$[Ni(Par)_2(H_2O)_2].\ 2H_2O$	Soln.-based	IS	S	S	S	IS	S	IS	S	S	IS
$[Fe(Par)_2(H_2O)_2]Cl.2H_2O$	Mech.	SS	S	S	S	IS	S	IS	SS	S	IS
$[Fe(Par)_2(H_2O)_2]Cl.2H_2O$	Soln.-based	SS	S	S	S	IS	S	IS	SS	S	IS
$[Cr(Par)_2(H_2O)_2]Cl.2H_2O$	Mech.	IS	IS	S	S	IS	S	IS	SS	S	IS
$[Cr(Par)_2(H_2O)_2]Cl.2H_2O$	Soln.-based	IS	IS	S	S	IS	S	IS	SS	S	IS

Key: S=soluble, SS=slightly soluble, IS=Insoluble

Table 4.1.4. Solubility of Aspirin and its Metal Complexes Synthesized by both Methods

Ligand / Compound	Method	Distilled Water	Ethanol	Methanol	Acetone	Chloroform	DEE	Petroleum Ether	DMF	DMSO	Nitrobenzene
Aspirin	-	SS	SS	S	IS	IS	SS	**IS**	**S**	S	IS
$[Cd(Asp)_2(H_2O)_2].2H_2O$	Mech	IS	IS	SS	SS	SS	SS	IS	S	S	IS
$[Cd(Asp)_2(H_2O)_2].2H_2O$	Soln.-based	IS	IS	SS	SS	SS	SS	IS	S	S	IS
$[Ni(Asp)_2(H_2O)_2].2H_2O$	Mech.	IS	S	S	S	S	S	IS	S	S	IS
$[Ni(Asp)_2(H_2O)_2].2H_2O$	Soln.-based	IS	S	S	S	S	S	IS	S	S	IS
$[Fe(Asp)_2(H_2O)_2]Cl.2H_2O$	Mech.	SS	SS	S	S	SS	S	IS	S	S	IS
$[Fe(Asp)_2(H_2O)_2]Cl.2H_2O$	Soln.-based	SS	SS	S	S	SS	S	IS	S	S	IS
$[Cr(Asp)_2(H_2O)_2]Cl.2H_2O$	Mech.	IS	IS	SS	S	SS	SS	IS	SS	S	IS
$[Cr(Asp)_2(H_2O)_2]Cl.2H_2O$	Soln.-based	IS	IS	SS	S	SS	SS	IS	SS	S	IS

Key: S=soluble, SS=slightly soluble, IS=Insoluble

Table 4.1.5. Magnetic Moment and Molar Conductivity of Paracetamol Metal Complexes Produced by Both Methods

Complex	Method	Magnetic Susceptibility(Xg) (g^{-1})	Molar Magnetic (Xm) (mol^{-1})	Effective Magnetic Moment (BM)	Molar Conductivity ($\Omega^{-1}g.dm^{-3}$)
$[Cd(Par)_2(H_2O)_2]$. $2H_2O$	Mech.	-6.330×10^{-7}	-3.072×10^{-4}	-	2.03×10^{-6}
$[Cd(Par)_2(H_2O)_2]$. $2H_2O$	Soln.	-6.182×10^{-7}	-3.000×10^{-4}	-	2.065×10^{-6}
$[Ni(Par)_2(H_2O)_2]$. $2H_2O$	Mech.	7.183×10^{-6}	3.105×10^{-3}	2.62	1.875×10^{-6}
$[Ni(Par)_2(H_2O)_2]$. $2H_2O$	Soln.	7.311×10^{-6}	3.161×10^{-3}	2.74	1.790×10^{-6}
$[Fe(Par)_2(H_2O)_2]Cl.2H_2O$	Mech.	2.870×10^{-5}	1.334×10^{-2}	5.64	3.945×10^{-6}

$[Fe(Par)_2(H_2O)_2]Cl.2H_2O$	Soln.	2.694×10^{-5}	1.252×10^{-2}	5.46	3.875×10^{-6}
$[Cr(Par)_2(H_2O)_2]Cl.2H_2O$	Mech.	2.223×10^{-5}	9.454×10^{-3}	4.75	2.085×10^{-6}
$[Cr(Par)_2(H_2O)_2]Cl.2H_2O$	Soln.	2.086×10^{-5}	8.872×10^{-3}	4.60	2.170×10^{-6}

Table 4.1.6. Effective Magnetic Moment and Molar Conductance of Aspirin Metal Complexes Synthesized by both Methods

Complex	Method	Magnetic Susceptibility(Xg) (g^{-1})	Molar Magnetic (Xm) (mol^{-1})	Effective Magnetic Moment (BM)	Molar Conductivity ($\Omega^{-1}gdm^{-3}$)
$[Cd(Asp)_2(H_2O)_2]$. $2H_2O$	Mech.	-4.48×10^{-7}	-2.434×10^{-4}	-	3.820×10^{-6}
$[Cd(Asp)_2(H_2O)_2]$. $2H_2O$	Solution	-4.52×10^{-7}	-2.456×10^{-4}	-	3.885×10^{-6}
$[Ni(Asp)_2(H_2O)_2]$. $2H_2O$	Mech.	7.034×10^{-6}	3.447×10^{-3}	2.87	2.510×10^{-6}
$[Ni(Asp)_2(H_2O)_2]$. $2H_2O$	Solution	7.029×10^{-6}	3.444×10^{-3}	2.87	2.470×10^{-6}
$[Fe(Asp)_2(H_2O)_2]Cl.2H_2O$	Mech.	2.739×10^{-5}	1.431×10^{-2}	5.84	3.850×10^{-6}
$[Fe(Asp)_2(H_2O)_2]Cl.2H_2O$	Solution	2.741×10^{-5}	1.433×10^{-2}	5.84	3.615×10^{-6}
$[Cr(Asp)_2(H_2O)_2]Cl.2H_2O$	Mech.	2.041×10^{-5}	9.864×10^{-3}	4.85	2.305×10^{-6}
$[Cr(Asp)_2(H_2O)_2]Cl.2H_2O$	Solution	2.028×10^{-5}	9.801×10^{-3}	4.83	2.265×10^{-6}

Table 4.1.7. The IR spectra of Paracetamol and its Metal Complexes Synthesized by both Methods

Ligand / Complex	Method	υ(N-H) cm^{-1}	υ(O-H) cm^{-1}	υ(N-H) cm^{-1} bend	υ(C=O)cm^{-1}	(M-N) cm^{-1}	(M-O) cm^{-1}
Paracetamol	-	3324	3106	-	1652	-	-
$[Cd(Par)_2(H_2O)_2$. $2H_2O$	Mech.	3387	3253	1566	1629	683	504

$[Cd(Par)_2(H_2O)_2].\ 2H_2O$	Soln.	3384	3167	1566	1638	683	508
$[Ni(Par)_2(H_2O)_2]\ .\ 2H_2O$	Mech.	3313	3180	1566	1655	680	503
$[Ni(Par)_2(H_2O)_2]\ .\ 2H_2O$	Soln.	3318	3151	1566	1655	679	503
$[Fe(Par)_2(H_2O)_2]Cl.2H_2O$	Mech.	3342	3168	1513	1656	677	503
$[Fe(Par)_2(H_2O)_2]Cl.2H_2O$	Soln.	3344	3212	1510	1655	679	504
$[Cr(Par)_2(H_2O)_2]Cl.2H_2O$	Mech.	3416	3162	1518	1643	681	503
$[Cr(Par)_2(H_2O)_2]Cl.2H_2O$	Soln.	3372	3240	1521	1639	681	503

Table 4.1.8. The IR Spectra of Aspirin and its Metal Complexes Synthesized by both Methods

Ligand / Complex	Method	υ(O-H) cm^{-1}	υ(C=O)cm^{-1} of ester	υ(C=O)cm^{-1} of carboxylic acid	(C-O) cm^{-1}	(C-O) cm^{-1}	(M-O) cm^{-1}
Aspirin	-	2866	1752	1680	1286	1095	-
$[Cd(Asp)_2(H_2O)_2]\ .\ 2H_2O$	Mech.	3227	1758	1685	1294	1097	511,
$[Cd(Asp)_2(H_2O)_2]\ .\ 2H_2O$	Soln.	3465	1756	1682	1298	1093	503,
$[Ni(Asp)_2(H_2O)_2]\ .\ 2H_2O$	Mech.	3331	1749	1685	1269	1097	444
$[Ni(Asp)_2(H_2O)_2]\ .\ 2H_2O$	Soln.	3334	1746	1686	1267	1097	503
$[Fe(Asp)_2(H_2O)_2]Cl\ .\ 2H_2O$	Mech.	3236	1755	1674	1295	1093	503
$[Fe(Asp)_2(H_2O)_2]Cl\ .\ 2H_2O$	Soln.	3233	1758	1679	1293	1092	503
$[Cr(Asp)_2(H_2O)_2]Cl\ .\ 2H_2O$	Mech.	3419	1761	1688	1285	1097	503

$[Cr(Asp)_2(H_2O)_2]Cl \cdot 2H_2O$	Soln.	3385	1759	1684	1284	1093	503

Table 4.1.9. Antibacterial Activity of Aspirin, Paracetamol and their Metal Complexes

Test Organism	Ligand / Complex	Inihibition Zone (mm) at different Concentration (µg/disc)			Control disc Cyproflaxicine (10 µg/disc)
		15	**30**	**60**	
Escherichia Coli	**Aspirin**	NZI	NZI	NZI	46
	$[Cd(Asp)_2(H_2O)_2].2H_2O$	10	10	18	
	$[Ni(Asp)_2(H_2O)_2].2H_2O$	NZI	14	28	
	$[Fe(Asp)_2(H_2O)_2]Cl.2H_2O$	NZI	NZI	NZI	
	$[Cr(Asp)_2(H_2O)_2]Cl.2H_2O$	12	14	18	
	Paracetamol	NZI	NZI	NZI	
	$[Cd(Par)_2(H_2O)_2].2H_2O$	NZI	8	12	
	$[Ni(Par)_2(H_2O)_2].2H_2O$	NZI	NZI	NZI	
	$[Fe(Par)_2(H_2O)_2]Cl.2H_2O$	NZI	NZI	NZI	
	$[Cr(Par)_2(H_2O)_2]Cl.2H_2O$	8	12	18	
Staphylococcus Aureus	**Aspirin**	NZI	NZI	NZI	32
	$[Cd(Asp)_2(H_2O)_2].2H_2O$	12	16	21	
	$[Ni(Asp)_2(H_2O)_2].2H_2O$	NZI	8	12	
	$[Fe(Asp)_2(H_2O)_2]Cl.2H_2O$	8	11	14	

$[Cr(Asp)_2(H_2O)_2]Cl.2H_2O$	NZI	12	18
Paracetamol	NZI	NZI	NZI
$[Cd(Par)_2(H_2O)_2].2H_2O$	NZI	8	12
$[Ni(Par)_2(H_2O)_2].2H_2O$	NZI	NZI	NZI
$[Fe(Par)_2(H_2O)_2]Cl.2H_2O$	NZI	NZI	NZI
$[Cr(Par)_2(H_2O)_2]Cl.2H_2O$	NZI	NZI	NZI

Key: NZI = No Zones of Inhibition

Table 4.2.1. Antifungal Activity of Aspirin, Paracetamol and their Metal Complexes

Test Organism	Ligand/Complex	Inihibition Zone (mm) at different Concentration (µg/disc)			Control disc Ketoconazole (10 µg/disc)
		15	**30**	**60**	
Mucus Specie	**Aspirin**	NZI	NZI	NZI	36
	$[Cd(Asp)_2(H_2O)_2].2H_2O$	NZI	18	28	
	$[Ni(Asp)_2(H_2O)_2].2H_2O$	NZI	8	12	
	$[Fe(Asp)_2(H_2O)_2]Cl.2H_2O$	NZI	NZI	NZI	
	$[Cr(Asp)_2(H_2O)_2]Cl.2H_2O$	NZI	NZI	NZI	
	Paracetamol	NZI	NZI	NZI	
	$[Cd(Par)_2(H_2O)_2].2H_2O$	NZI	NZI	NZI	
	$[Ni(Par)_2(H_2O)_2].2H_2O$	NZI	NZI	NZI	

	$[Fe(Par)_2(H_2O)_2]Cl.2H_2O$	NZI	NZI	NZI	
	$[Cr(Par)_2(H_2O)_2]Cl.2H_2O$	NZI	NZI	NZI	
Candida	**Aspirin**	NZI	NZI	NZI	41
	$[Cd(Asp)_2(H_2O)_2].2H_2O$	16	28	31	
	$[Ni(Asp)_2(H_2O)_2].2H_2O$	NZI	26	31	
	$[Fe(Asp)_2(H_2O)_2]Cl.2H_2O$	22	32	40	
	$[Cr(Asp)_2(H_2O)_2]Cl.2H_2O$	28	32	38	
	Paracetamol	NZI	NZI	NZI	
	$[Cd(Par)_2(H_2O)_2].2H_2O$	NZI	NZI	14	
	$[Ni(Par)_2(H_2O)_2].2H_2O$	NZI	10	14	
	$[Fe(Par)_2(H_2O)_2]Cl.2H_2O$	NZI	NZI	NZI	
	$[Cr(Par)_2(H_2O)_2]Cl.2H_2O$	20	24	38	

Key: NZI = No Zones of Inhibition

Table 4.2.2. Mole Ratio of Metal : Ligand in the Complexes using Job's Method

Complex	X	1 - X	n = X/(1 - X)
$[Cd(Asp)_2(H_2O)_2] . 2H_2O$	0.6	0.40	1.5 ≈ 2
$[Ni(Asp)_2(H_2O)_2] . 2H_2O$	0.61	0.39	1.56 ≈ 2
$[Fe(Asp)_2(H_2O)_2]Cl .2H_2O$	0.61	0.39	1.56 ≈ 2
$[Cr(Asp)_2(H_2O)_2]Cl .2H_2O$	0.61	0.39	1.56 ≈ 2

$[Cd(Par)_2(H_2O)_2]$. $2H_2O$	0.61	0.39	1.56 ≈ 2
$[Ni(Par)_2(H_2O)_2]$. $2H_2O$	0.6	0.40	1.5 ≈ 2
$[Fe(Par)_2(H_2O)_2]Cl$.$2H_2O$	0.61	0.39	1.56 ≈ 2
$[Cr(Par)_2(H_2O)_2]Cl$.$2H_2O$	0.61	0.39	1.56 ≈ 2

Table 4.2.3. Determination of Water of Hydration In The Paracetamol Complexes

Complex	Initial mass (g)	Final mass (g)	Loss in mass	% of water
$[Cd(Asp)_2(H_2O)_2]$. $2H_2O$	0.2	0.191	0.009	4.5
$[Cd(Asp)_2(H_2O)_2]$. $2H_2O$	0.2	0.187	0.013	6.5
$[Ni(Asp)_2(H_2O)_2]$. $2H_2O$	0.2	0.189	0.011	5.5
$[Ni(Asp)_2(H_2O)_2]$. $2H_2O$	0.2	0.186	0.014	7.0
$[Fe(Asp)_2(H_2O)_2]Cl$. $2H_2O$	0.2	0.190	0.010	5.0
$[Fe(Asp)_2(H_2O)_2]Cl$. $2H_2O$	0.2	0.187	0.013	6.5
$[Cr(Asp)_2(H_2O)_2]Cl$. $2H_2O$	0.2	0.189	0.011	5.5
$[Cr(Asp)_2(H_2O)_2]Cl$. $2H_2O$	0.2	0.185	0.015	7.5

Table 4.2.4. Determination of Water of Hydration In The Aspirin Complexes

Complex	Initial mass (g)	Final mass (g)	Loss in mass	% of water
$[Cd(Asp)_2(H_2O)_2]$. $2H_2O$	0.2	0.189	0.011	5.5
$[Cd(Asp)_2(H_2O)_2]$. $2H_2O$	0.2	0.185	0.015	7.5

$[Ni(Asp)_2(H_2O)_2]$. $2H_2O$	0.2	0.188	0.012	6.0
$[Ni(Asp)_2(H_2O)_2]$. $2H_2O$	0.2	0.186	0.014	7.0
$[Fe(Asp)_2(H_2O)_2]Cl$. $2H_2O$	0.2	0.190	0.010	5.0
$[Fe(Asp)_2(H_2O)_2]Cl$. $2H_2O$	0.2	0.187	0.013	6.5
$[Cr(Asp)_2(H_2O)_2]Cl$. $2H_2O$	0.2	0.191	0.009	4.5
$[Cr(Asp)_2(H_2O)_2]Cl$. $2H_2O$	0.2	0.187	0.013	6.5

Table 4.2.5. Gravimetric Analysis Data for Paracetamol Complexes

Metal	Method	Weight of complex used (g)	Gravimetric factor (g)	Weight of prdt obtained (g)	Average Wght of prdt (g)	% Composition of Metal (g.mol^{-1})	
						Calculated	Observed
$[Cd(Asp)_2(H_2O)_2]$. $2H_2O$	Mech.	0.2	0.2463	0.1674	0.0412	23.15	20.60
$[Cd(Asp)_2(H_2O)_2]$. $2H_2O$	Soln.	0.2	0.2463	0.1746	0.0430	23.15	21.50
$[Ni(Asp)_2(H_2O)_2]$. $2H_2O$	Mech.	0.2	0.2251	0.1102	0.0248	13.58	12.40
$[Ni(Asp)_2(H_2O)_2]$. $2H_2O$	Soln.	0.2	0.2251	0.1150	0.0259	13.58	12.95
$[Fe(Asp)_2(H_2O)_2]Cl.2H_2O$	Mech.	0.2	0.3497	0.0668	0.0234	12.02	11.70
$[Fe(Asp)_2(H_2O)_2]Cl.2H_2O$	Soln.	0.2	0.3497	0.0688	0.0241	12.02	12.05
$[Cr(Asp)_2(H_2O)_2]Cl.2H_2O$	Mech.	0.2	0.1609	0.1538	0.0247	13.93	12.35
$[Cr(Asp)_2(H_2O)_2]Cl.2H_2O$	Soln.	0.2	0.1609	0.1584	0.0255	13.93	12.75

Table 4.2.6. Gravimetric Analysis Data for Aspirin Metal Complexes

Metal	Method	Weight of complex used (g)	Gravimetr-ic factor (g)	Weight of prdt obtained (g)	Average wght of prdt (g)	% Composition of Metal (X_g) x 10^{-3} (mol^{-1})	
						Calculated	Observed
$[Cd(Asp)_2(H_2O)_2]$. $2H_2O$	Mech.	0.2	0.2463	0.1724	0.0425	20.69	21.25
$[Cd(Asp)_2(H_2O)_2]$. $2H_2O$	Soln.	0.2	0.2463	0.1783	0.0439	20.69	21.95
$[Ni(Asp)_2(H_2O)_2]$. $2H_2O$	Mech.	0.2	0.2033	0.1146	0.0233	11.98	11.65
$[Ni(Asp)_2(H_2O)_2]$. $2H_2O$	Soln.	0.2	0.2033	0.1137	0.0230	11.98	11.50
$[Fe(Asp)_2(H_2O)_2]Cl.2H_2O$	Soln.	0.2	0.3497	0.0646	0.0226	11.46	11.30
$[Fe(Asp)_2(H_2O)_2]Cl.2H_2O$	Soln.	0.2	0.3497	0.0579	0.0202	10.69	10.10
$[Cr(Asp)_2(H_2O)_2]Cl.2H_2O$	Mech.	0.2	0.1609	0.1301	0.0209	10.76	10.45
$[Cr(Asp)_2(H_2O)_2]Cl.2H_2O$	Soln.	0.2	0.1609	0.1315	0.0212	10.76	10.60

4. Discussion

The mechanochemical solid-state synthesis method used in this study produced the desired products in approximately 5 minutes, a significant improvement over the conventional solution-based reflux method, which typically requires several hours or even days. The analytical data for the metal complexes of both paracetamol and aspirin, synthesized by these two methods, were comparable, although there were differences in yield percentages. The complexes formed via the mechanochemical method were notably more productive, with yields ranging from 87.42 % to 91.00 %, compared to the solution-based method's yields of 66.84 % to 69.21 %. Most of the synthesized complexes, except those with cadmium, exhibited color due to electronic transitions of eg and t2g electrons. Additionally, paracetamol itself decomposed at 170 °C, while its metal complexes had decomposition temperatures between 187.6 °C and 198.3 °C, indicating successful coordination with metal ions and enhanced stability, as detailed in Table 4.1.1.

Aspirin decomposes at 137 °C, whereas its metal complexes have higher decomposition temperatures, ranging from 164.5 °C to 181.3 °C, regardless of whether they were synthesized via mechanochemical or solvent-based methods, as shown in Table 4.1.2. This increase in decomposition temperature suggests effective coordination between the ligand and the metal ions.

Paracetamol exhibits slight solubility in water, acetone, chloroform, diethyl ether (DEE), and petroleum ether (PE) at room temperature, but it dissolves well in ethanol, methanol, DMF, and DMSO, and is insoluble in nitrobenzene and formaldehyde. Its metal complexes are soluble in acetone, methanol, DMF, DMSO, and DEE. Aspirin is soluble in methanol, DMF, and DMSO, but its complexes are generally insoluble in water, except for Cr(III) complexes. The differences in solubility can be attributed to the non-polar nature of metal(II) complexes and the slightly polar nature of metal(III) complexes.

Table 4.1.5 displays the magnetic properties of paracetamol metal complexes. According to the magnetic susceptibility measurements, Cd(II) paracetamol complexes are diamagnetic, while Ni(II), Fe(III), and Cr(III) complexes, synthesized by both mechanochemical and solution-based methods, are paramagnetic. The paramagnetic behavior is attributed to the presence of unpaired electrons in the partially filled d-orbitals of the central metal ions (Adesina, 2008), whereas diamagnetism is due to all electrons being paired in the d-orbital.

The magnetic moment values, which can also indicate the likely geometry of the complexes, are detailed in Table 4.1.5. At room temperature, the effective magnetic moments for the paracetamol metal complexes were consistent across both synthesis methods. For Ni(II), Fe(III), and Cr(III) complexes, the magnetic moments ranged from 2.62 BM to 2.74 BM, 5.64 BM to 5.46 BM, and 4.75 BM to 4.60 BM, respectively. No magnetic moment was recorded for the Cd(II) complexes in this study.

The effective magnetic moment values of 4.75 BM and 4.60 BM observed for Cr(III) paracetamol complexes are higher than the spin-only magnetic moment range (3.7-3.9 BM) for a high-spin octahedral geometry, as noted by LibreTexts (2015). This supports the proposal that these complexes have a high-spin octahedral structure.

For Ni(II) paracetamol complexes, the magnetic moments of 2.62 BM and 2.74 BM, obtained from mechanochemical and solution-based methods respectively, suggest a tetrahedral geometry (Adekunle, 2013).

The effective magnetic moments for Fe(III) paracetamol complexes, recorded as 5.64 BM and 5.46 BM, fall within the expected range for high-spin octahedral geometry. This aligns with Adekunle's (2013) findings. Deviations from spin-only values may be attributed to spin-orbit coupling.

For aspirin complexes, similar μeff values were observed for both mechanochemical and solution methods, with all complexes except Cd(II) being paramagnetic. $Cd(asp)_2(H_2O)_2$ is diamagnetic due to the lack of unpaired electrons in the cadmium(II)

ion's d-orbital. Effective magnetic moment data for aspirin complexes are summarized in Table 4.1.6, with no values for Cd(II) aspirin complexes in this study (Yousif et al., 2013).

Ni(II) aspirin complexes showed magnetic moments of 2.87 BM for both methods, indicating high-spin tetrahedral geometry, though slightly higher than the spin-only value of 2.83 BM, possibly due to orbital effects (El-Halawa, 2015).

For Fe(III) aspirin complexes, the observed μeff of 5.84 BM for both methods suggests an octahedral geometry. Cr(III) aspirin complexes displayed μeff values of 4.85 BM and 4.83 BM, which fall within the expected range (4.7-4.9 BM) for high-spin octahedral geometry around Cr(III) ions, as reported by LibreTexts (2015).

Table 4.1.5 shows the molar conductance values of paracetamol complexes in 1×10^{-3} M DMSO at room temperature. The conductance values for the mechanochemical and solution-based products are similar. Specifically, the molar conductance for Cd(II), Ni(II), Fe(III), and Cr(III) paracetamol complexes ranges from 2.03×10^{-6} to 3.945×10^{-6} $\Omega^{-1}cm^2mol^{-1}$ for mechanochemical products and from 2.065×10^{-6} to 3.875×10^{-6} $\Omega^{-1}cm^2mol^{-1}$ for solution-based products. These values fall within the expected range for non-electrolytes in DMSO, as reported by Adekunle (2013).

Table 4.1.6 presents the molar conductance of aspirin metal complexes in 1×10^{-3} M DMSO at room temperature. The conductance values for both mechanochemical and solution-based products range from 94.40 to 207.61 $\Omega^{-1}cm^2mol^{-1}$. Specifically, the molar conductance values for Cd(II), Ni(II), Fe(III), and Cr(III) aspirin complexes are 3.820×10^{-6} to 3.885×10^{-6} $\Omega^{-1}cm^2mol^{-1}$ for mechanochemical products and 2.510×10^{-6} to 2.470×10^{-6} $\Omega^{-1}cm^2mol^{-1}$ for solution-based products. This range indicates that the complexes are also non-electrolytes in DMSO, according to Adekunle (2013).

Table 4.1.7 shows the IR spectral data for paracetamol and its metal complexes. In free paracetamol, the absorption band at 3324 cm^{-1} is attributed to the N-H vibration. This band shifts to 3313-3387 cm^{-1} in the metal complexes, indicating coordination of the paracetamol nitrogen with the central metal ion. New peaks appearing in the range of 677-683 cm^{-1} in the complexes confirm the formation of M-N bonds (Fugu et al., 2013). The band at 3106 cm^{-1} corresponds to the O-H vibration of the phenolic group in paracetamol.

The observed smaller BM values and the size of Ni^{2+} and Cd^{2+} ions suggest a tetrahedral structure for their complexes. In contrast, the larger Fe^{3+} and Cr^{3+} ions and higher BM values, along with the C=O band shifting to a lower range, indicate an octahedral geometry for their complexes. The disappearance of the phenolic O-H band suggests coordination through phenolic oxygen after deprotonation, supported by new bands at 503-508 cm^{-1} due to M-O bonding.

The IR spectra of the complexes also show bands in the 3144-3389 cm^{-1} range, indicating the presence of coordinated water molecules (Aliyu et al., 2009).

In free aspirin, the absorption band at 2866 cm^{-1} corresponds to the O-H vibration of the carboxylic group. This band disappears in the metal complexes, suggesting that the O-H group is involved in coordination. The bands at 1752 cm^{-1} and 1680 cm^{-1} for ester and carboxylic acid C=O vibrations shift to 1659-1758 cm^{-1} in the complexes, indicating these groups are also coordination sites. The C-O stretching vibrations of the carboxylic and ester groups in aspirin shift to 1295-1267 cm^{-1} and 1097-1093 cm^{-1}, respectively, supporting the formation of new compounds. Bands at 444-503 cm^{-1}, not present in the free aspirin spectrum, are attributed to M-O stretching vibrations, further supporting the coordination of aspirin with the metal ions.

The IR spectra of the metal complexes reveal bands in the 3144-3389 cm^{-1} range, which are not present in the free aspirin spectra, indicating the presence of coordinated water molecules (Aliyu et al., 2009).

Antimicrobial testing results for the drugs and their metal complexes against *Escherichia coli*, *Staphylococcus aureus*, *Mucor species*, and *Candida* are summarized in Tables 4.1.9 and 4.2.1. The ligands themselves showed no activity against these bacteria and fungi at any concentration. Among the paracetamol complexes, only $[Cd(par)_2(H_2O)_2]\cdot2H_2O$ and

$[Cr(par)_2(H_2O)_2]Cl{\cdot}2H_2O$ displayed minimal activity against *Escherichia coli* and *Staphylococcus aureus* at higher concentrations. Specifically, $[Cr(par)_2(H_2O)_2]Cl{\cdot}2H_2O$ was inactive against *Staphylococcus aureus* at all tested concentrations and showed no activity against *Mucor species*. However, $[Cr(par)_2(H_2O)_2]Cl{\cdot}2H_2O$ demonstrated significant antifungal activity against *Candida* across all concentrations, while $[Ni(par)_2(H_2O)_2]{\cdot}2H_2O$ showed low activity at higher concentrations and $[Fe(par)_2(H_2O)_2]Cl{\cdot}2H_2O$ showed no activity.

For aspirin complexes, there was low to moderate activity against *Escherichia coli* and *Staphylococcus aureus*. The Fe(III) and Cr(III) aspirin complexes did not inhibit *Mucor species*, whereas Cd(II) and Ni(II) complexes produced inhibition zones ranging from 8 mm to 28 mm at various concentrations. Antifungal activity against *Candida* was better, with inhibition zones ranging from 16 mm to 40 mm across different concentrations for Cd(II), Ni(II), Fe(III), and Cr(III). $[Ni(Asp)_2(H_2O)_2]{\cdot}2H_2O$ showed no activity at the lowest concentration (15 μg/disc).

Overall, metal complexes generally exhibited greater effectiveness than the free ligands. This enhanced activity is likely due to chelation, which decreases the metal atom's polarity and increases its lipophilicity, aiding its penetration through bacterial and fungal membranes. The variation in activity among the complexes may be due to their lipophobic nature and the fact that aspirin and paracetamol are bacteriostatic (Aderoju and Abiodun, 2016).

Based on melting point, conductivity, magnetic susceptibility, Job's method, and FTIR data, tentative structures for the metal complexes of paracetamol and aspirin are proposed.

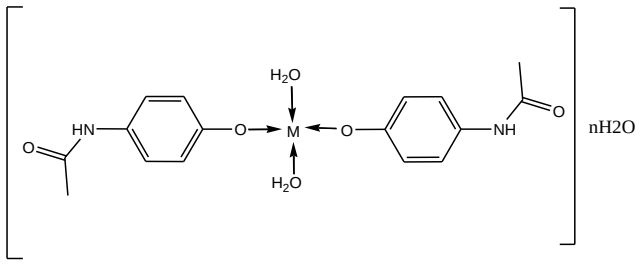

Figure 4.1. Proposed structure for $[M(Par)_2(H_2O)_2] \cdot nH_2O$
M = Ni(II) and Cd(II) ions
n = 2

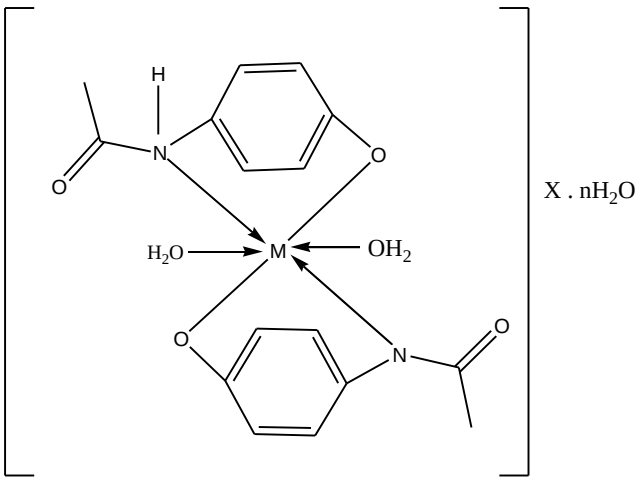

Figure 4.2. Proposed structure for $[M(Par)_2(H_2O)_2]X \cdot 2H_2O$
M = Fe(III) and Cr(III) ions
X = Cl, n = 2

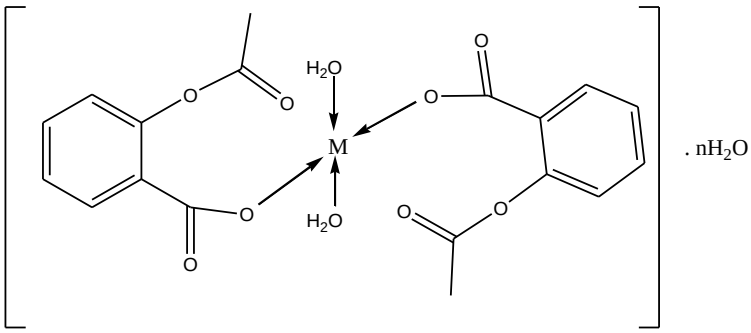

Figure 4.3. Proposed structure for $[M(Asp)_2(H_2O)_2] . nH_2O$

M = Ni(II) and Cd(II) ions

n = 2

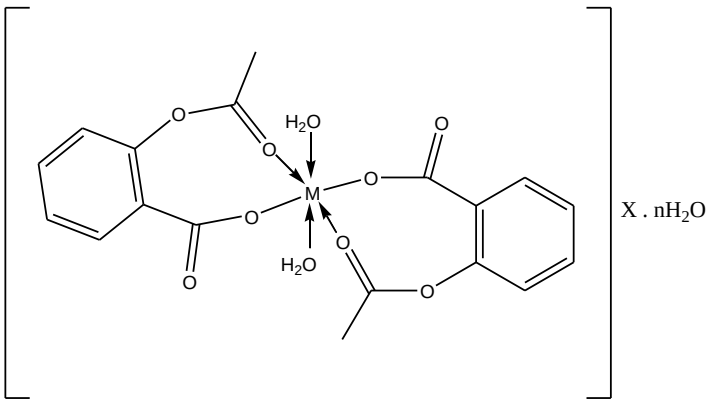

Figure 4.4. Proposed structure for $[M(Asp)_2(H_2O)_2]X . nH_2O$

M = Fe(III) and Cr(III) ions

X = Cl, n = 2

5. Conclusion

The study successfully synthesized and characterized complexes of divalent and trivalent transition metals with aspirin and paracetamol. These complexes were stable and demonstrated effectiveness against the tested bacterial and fungal species, unlike the parent drugs, which showed no activity.

The research highlighted the advantages of mechanochemical synthesis over traditional solution-based methods, suggesting that scientists worldwide should consider adopting this efficient synthetic approach for preparing complexes and other compounds.

6. Recommendations

For comprehensive characterization of these complexes, additional analyses such as single crystal structure determination, X-ray powder diffraction, and NMR spectroscopy (^1H and ^{13}C) are recommended.

Given that some synthesized complexes exhibited significant activity against specific microorganisms, further testing with a broader range of bacterial and fungal species is advised to explore potential enhanced inhibitory effects against other pathogens.

7. Declaration

The authors declared that there is no conflict of interest.

REFERENCES

Adams, C. J., Haddow, M. F., Hughes, R. J. L., Kurawa, M. A., & Orpen, A. G. (2010). Coordination Chemistry of Platinum and Palladium in the Solid-State: Synthesis of Imidazole and Pyrazole Complexes. *Dalton Transactions, 39*(1), 3714-3724.

Adams, C. J., Orpen, A. G., & Kurawa, M. A. (2010). Coordination Chemistry in the Solid State: Reactivity of Manganese and Cadmium Chlorides with Imidazole and Pyrazole and Their Hydrochlorides. *Inorganic Chemistry, 49*(22), 10475-10485.

Adekunle, F. A. O. (2013). Ni(II), Co(II), Mn(II) and Zn(II) Complexes of 5,6-Dihydro-5,6-Epoxy-1,10-Phenanthroline: Synthesis and Spectroscopy Studies. *International Journal of Basic and Applied Sciences, 13*(3), 130403-9292.

Adzila, S., Sopyan, L., & Handi, M. (2012). Mechanochemical Synthesis of Hydroxyapatite Nanopowder: Effect of Rotation Speed and Milling Time on Powder Properties. *Applied Mechanics and Materials, 110-116*(1), 3632. https://doi.org/10.4028/www.scientific.net/AMM.110-116.3632

Agbaje, O. B. A., Wakil, S. M., & Osowole, A. A. (2014). Synthesis, Spectroscopic Characterization, and Antimicrobial Activities of Some Mixed Drug Metal (II) Complexes of Sulfamethoxazole and Paracetamol. *Journal of Chemical Research, 1*(1), 1–18.

Ahluwalia, V. K., & Kidwai, M. (2004). New Trends in Green Chemistry: Organic Synthesis in Solid State. *Kluwer Academic Publishers.*

Ahmad, J. (2010). Hepatology and Transplant Hepatology: A Case-Based Approach. *Springer, 194.*

Aliyu, H. N., & Abdullahi, H. J. (2009). Synthesis and Characterization of Manganese(II), Cobalt(II), Nickel(II), and Copper(II) N,N′-Bis(Benzoin)Ethylenediiminato Complexes. *Bayero Journal of Pure and Applied Sciences, 2*(1), 110-112.

Al Noor, T. H., Ghanim, F. H., & Kindeel, A. S. (2014). Synthesis, Characterization, and Antibacterial Activity of Mn(II), Fe(II), Ni(II), Cu(II), Zn(II), Cd(II), and Hg(II) Mixed-Ligand Complexes Containing Fural-2-Carboxylic Acid and 1,10-Phenanthroline. *Advances in Physics Theories and Applications, 29*(1), ISSN 2224-719X.

Amer, J., Hadi, D., Nur, H., & Hermawan, H. (2015). Structure-Property Relationships of Iron-Hydroxyapatite Ceramic Matrix Nanocomposite Fabricated Using Mechanosynthesis Method. *Materials Science and Engineering C, 51*(1), 294–299. https://doi.org/10.1016/j.msec.2015.03.019

Amin, M. (2014). One-Pot Solvent-Free Synthesis, Cytotoxicity, and In Vitro Urease Inhibitory Activity of Zinc (II)-Piroxicam Complex. *World Journal of Pharmacy and Pharmaceutical Sciences, 3*(4), 89-99.

Amudat, A., & Obaleye, J. (2007). Synthesis, Characterization, and Antibacterial Activity of Aspirin and Paracetamol-Metal Complexes. *Biokemistri, 19*(1), 9-15.

Balaz, P. (2008). Mechanochemistry in Nanoscience and Minerals Engineering. *Springer.*

Benista, M. J., & Nowak, J. Z. (2014). Paracetamol: Mechanism of Action, Applications, and Safety Concerns. *Acta Poloniae Pharmaceutica - Drug Research, 71*(1), 11–23.

Bergmann, I., Diekmann, A., Heitjans, P., & Becker, K. D. (2008). Mechanosynthesis of Nanocrystalline Iron Germanate Fe2GeO4 with a Nonequilibrium Cation Distribution. *Solid State Ionics, 18*(1), 349–352.

Boudeville, P., Vert, M., El Briak-BenAbdeslam, H., & Ginebra, M. P. (2007). Wet or Dry Mechanochemical Synthesis of Calcium Phosphate? Influence of the Water Content on DCPD-CaO Reaction Kinetics. *Acta Materialia Inc., 1*(1), 378-386.

Braga, D., Grepioni, F., Maini, L., Brescello, R., & Catairea, L. (2008). Cryst. Eng. Comm. *Journal of Materials Chemistry, 10*(1), 469-471.

British National Formulary. (2003). British Medical and Royal Pharmaceutical Society of Great Britain. 45th ed.

British National Formulary for Children. (2006). British Medical Journal and Royal Pharmaceutical Society.

Burgess, J. (1978). Metal Ions in Solution. *John Wiley & Sons, Inc.*

Cisneros-de, R., Cero, R., Beltra, H. I., Soto-Castruita, E., & Pons-Jiménez, M. (2016). Solid and Liquid Supramolecular Complexes by Solid-Solid Mechanosynthesis. *Arabian Journal of Chemistry, 1*(1), http://dx.doi.org/10.1016/j.arabjc.2016.08.008.

Chandrathilaka, A. M. D. S., Hettiarachchi, C. V., & Ileperuma, O. A. (2013). Spectrophotometric and pH Metric Studies on Pb(II), Cd(II), Al(III), and Cu(II) Complexes of Paracetamol and Ascorbic Acid. *Journal of the National Science Foundation of Sri Lanka, 41*(4), 337-344.

Chou, R., & Huffman, L. H. (2007). Medication for Acute and Chronic Low Back Pain: A Review of the Evidence for an American Pain Society/American College of Physicians Clinical Practice Guideline. *Annals of Internal Medicine, 147*(7), 505-514.

Cortés-Escobedo, C. A., Bolarín-Miró, A. M., Jesús, F. S., Valenzuela, R., Juárez-Camacho, E. P., Samperio-Gómez, I. L., & Ammar, S. (2013). Y3Fe5O12 Prepared by Mechanosynthesis from Different Iron Sources. *Materials Chemistry and Physics, 1*(1), 41-46.

Cristovoa, B. (2011). Spectral, Thermal, and Magnetic Properties of Cu(II) and Ni(II) Complexes with Schiff Base Ligands. *Journal of the Serbian Chemical Society, 76*(12), 1639-1648.

Daly, F. F., Fountain, J. S., Murray, L., Graudins, A., & Buckley, N. A. (2008). Guidelines for the Management of Paracetamol Poisoning in Australia and New Zealand: Explanation and Elaboration. A Consensus Statement from Clinical Toxicologists Consultant to the Australian Poisons Information Centers. *Medical Journal of Australia, 188*(5), 296-301.

Prochowicz, D., Franckevičius, M., Cieślak, S., Zakeeruddin, M. L., & Grätzel, J. (2016). Mechanosynthesis of the Hybrid Perovskite CH3NH3PbI3: Characterization and the Corresponding Solar Cell Efficiency. *Journal of Materials Chemistry, 3*(1), 1-7.

Dostál, J., Paulová, H., Táborská, E., & Tomandl, J. P. D. (2014). *Essentials of medical chemistry and biochemistry*. Brno.

Ferna, F. (1999). Mechanochemistry: An overview. *Pure and Applied Chemistry, 17*(4), 581–586.

Friš, T. (2013). Mechanochemistry: From solvent-free, low-energy synthesis to (photo- or thermo-) chemically-driven mechanical motion.

El-Halawa, R. A., Mahal, A., Zabin, S. A., Ibrahim, M., Al-Refai, M., & Kaimari, T. (2015). Synthesis, characterization, and antifungal activity of some metal complexes derived from quinoxaloylhydrazone. *World Journal of Organic Chemistry, 3*(1), 1-8.

Friscic, T., Halasz, I., Strukil, V., Maksic, M. E., & Dinnebier, R. E. (2012). Clean and efficient synthesis using mechanochemistry: Coordination polymers, metal-organic frameworks, and metallodrugs. *Croatica Chemica Acta, 85*(3), 367-378.

Garay, A. L., Pichon, A., & James, S. L. (2007). Opportunity for new and cleaner synthesis. *Chemical Society Reviews*, 846-855.

Hassan, S. W., Umar, R. A., Lawal, M., Bilbis, L. S., & Muhammed, B. Y. (2006). Evaluation of antifungal activity of *Ficus sycomorus* L. (*Moraceae*). *Best Journal, 3*(2), 18-25.

Heinike, G. (1984). *Tribochemistry*. Academie-Verlag.

Holleman, A. F., Wiberg, E., & Wiberg, N. (1985). Zink. *Lehrbuch der Anorganischen Chemie*. Walter de Gruyter, 1034-1041. ISBN 3-11-007511-3.

Iurowa, K. W. I., & Amrat, K. G. (2007). Some aspects of mechanochemical reactions. *Materials Science-Poland, 25*(1).

James, S. L., Adams, C. J., Bolm, C., Braga, D., & Waddell, D. C. (2012). Mechanochemistry: Opportunities for new and cleaner synthesis. *Chemical Society Reviews, 41*(413-447).

Hernandez, J., & Bolm, C. (2015). [Cp*RhCl2]2: Mechanosynthesis and applications in C–H bond functionalizations under ball-milling conditions. *Chemical Communications, 51*(12582-12584). The Royal Society of Chemistry.

Karthikeya, M., Glen, R. C., & Bend, A. (2005). General melting point prediction based on a diverse compound data set and artificial neutral network. *Journal of Chemical Information and Modeling, 45*(3), 581-590.

Kaupp, G. (2009). Mechanochemistry: The varied application of mechanical bond-breaking. *CrystEngComm, 11*(388-403).

Kaupp, G. (2006). *CrystEngComm, 8*(794-804).

Kurawa, M. A., & Yammama, S. G. (2014). Solid state synthesis, characterization, and antimicrobial study of 4,4'-bipyridinecopper (II) complexes. *ChemSearch Journal, 5*(2), 39-45.

Kurawa, M. A., & Yammama, S. G. (2014). Solid state synthesis, characterization, and biological activity of 4,4'-bipyridiniumtetrachloronickelate (II) and 4,4'-bipyridine dichloronickel (II) complexes. *ChemSearch Journal, 5*(1), 59-65.

Kurawa, M. A., & Adams, C. J. (2015). Solid state synthesis and single crystal X-ray crystallographic analysis of 2-oxo-2,3-dihydropyrimidin-1-ium{trichloridopyrimidin-2(1H)-one}cobaltate (II) [H2pyrno][CoCl3(Hpymo)]. *ChemSearch Journal, 6*(1), 52-56.

Kurawa, M. A., & Orpen, A. G. (2015). Synthesis and single crystal X-ray structure determination of bis-3,3',5,5'-tetramethyl-4,4'-bipyrazoliumtetrachloromanganate (II) monohydrate [H2Me4bpz]2[MnCl4]Cl2.H2O. *ChemSearch Journal, 6*(1), 68-73.

Lewis, H. D., Davis, J. W., Archibad, D. G., Demots, H. (1983). Protective effect of aspirin against acute myocardial infection and death in men with unstable angina: Results of the Veterans Administration Cooperative Study. *The New England Journal of Medicine, 309*(7), 396-403.

Livingstone, F. B. (1985). Frequencies of hemoglobin variant: Thalassemia, the glucose-6-phosphate dehydrogenase deficiency, G6PD variants, and ovalocytosis in human populations. *Oxford University Press*.

Lusi, M., Adams, C. J., Kurawa, M. A., & Orpen, A. G. (2009). Solid state synthesis of coordination compounds from basic metal salts. *CrystEngComm, 10*(12), 1790-1795.

Masram, D. T., & Debnath, A. (2013). Synthesis and characterization of some transition metal complexes of norfloxacin in the presence of 1,10-phenanthroline. *Der Pharma Chemica, 5*(5), 285-290.

Mochales, C., Briak-benabdeslam, H. E., Pau, M., Terol, A., Planell, J. A., & Boudeville, P. (2004). Dry mechanochemical synthesis of hydroxyapatites from DCPD and CaO: Influence of instrumental parameters on the reaction kinetics. *Biomaterials, 25*(1151–1157).

Mottillo, C., Lu, Y., Pham, M., & Do, T. (2013). Mineral neogenesis as an inspiration for mild, solvent-free synthesis of bulk microporous metal–organic frameworks from metal (Zn, Co) oxides. *Green Chemistry*, 15(8), 2121–2131.

Nasiri-Tabrizi, B., Adhami, T., & Ebrahimi-Kahrizsangi, R. (2014). Effect of processing parameters on the formation of TiB2 nanopowder by mechanically induced self-sustaining reaction. *Ceramics International*, 40(5), 7345-7354.

Obaleye, J. A., & Lawal, A. (2007). Synthesis, characterization and antibacterial activity of aspirin and paracetamol metal complexes. *Journal of BIOKEMISTRI*, 19(1), 9-15.

Odesina, I. A. (2008). *Essential Chemistry for Senior Secondary Schools* (2nd ed.). Ibafo, Ogun State: TONAD Publishers Limited.

Olmos, A. R. V., Osorio, A. L. F., Ramos-Bautista, F., & Sato-Berrú, R. (2008). Nano science and nano technology: An Indian journal. *Nano Science and Nano Technology*, 2(1).

Orpen, A. G., Adams, C. J., & Kurawa, M. A. (2010). Coordination chemistry in the solid state: Synthesis and interconversion of pyrazolium salts, pyrazole complexes, and pyrazolate MOF. *Dalton Transactions*, 39(31), 6974-6984.

Orpen, A. G., Adams, C. J., Kurawa, M. A., & Lusi, M. (2008). Solid state synthesis of coordination compounds from basic metal salts. *CrystEngComm*, 10(12), 1790-1795.

Osowole, A. A., Agbaje, O. B. A., & Wakil, S. S. (2015). Synthesis, characterization and biological activity of paracetamol and benzoic acid. *International Journal of Applied Medical Science*, 1(2), 77-87.

Othman, R., Xuan, N., Tram, T., Fauzi, A., & Noor, M. (2013). Dry mechanosynthesis of carbonate-substituted hydroxyapatite. *Journal of Materials Science and Engineering*, 2(2), 18–27.

Palleros, D. R. (2000). *Experimental Organic Chemistry*. New York: John Wiley & Sons.

Pymo, Z., & Kurawa, M. A. (2012). Synthesis and structural analyses of bis(2-oxo-2,3-dihydropyrimidin-1-ium) tetrachlorozincate(II) [H2Pymo][ZnCl4] and bis(pyrimidin-2-olate) zinc(II). *Journal of Inorganic Chemistry*, 3(2), 1–7.

Raithel, M., Baenkler, H. W., Naegel, A., Buchwald, F., Schultis, H. W., Backhaus, B., Kimpel, S., Koch, H., Mach, K., Hahn, E. G., & Konturek, P. C. (2005). Significance of salicylate intolerance in disease of the lower gastrointestinal tract. *Journal of Physiology and Pharmacology*, 56(5), 89-102.

Rao, P. V., Ashwini, K., & Ammani, S. (2007). Synthesis and characterization of transition metal complexes derived from some biologically active furoic acid hydrazones. *Bulletin of the Chemical Society of Ethiopia*, 21(1), 63-73.

Arribas-Bueno, R., Murphy, B., Verma, V., Crowley, C., Davern, P., & Synthesis, S. H. K. H. (2016). The crystallization of active pharmaceutical ingredients (APIs) onto excipient matrices. *Journal of Pharmaceutical Research*, 32(4), 1020-1027.

Rechenberg, H. R. (2000). Mechanosynthesis of intermetallic Fe100−xAlx obtained by reduction of Al/Fe2O3 composite. *Journal of Physics: Condensed Matter*, 12(45), 10579–10590.

Refat, M. S., El-korashy, S. A., & Hussien, M. A. (2014). Ligational, spectroscopic (infrared and electronic) and thermal studies on the Mn(II), Co(II), Fe(II) and Cu(II) complexes with analgesic drugs. *Journal of Canadian Chemical Transactions*, 2(1), 24-35.

Senna, G. E., Andri, G., Dama, A. R., Mezzelani, P., & Andri, L. (1995). Tolerability of imidazole salicylate in aspirin-sensitive patients. *Allergy Proceedings*, 16(5), 251-254.

Shah, M., & Sharma, A. (2013). Synthesis and characterization of some transition metal complexes derived from bidentate Schiff base ligand. *IOSR Journal of Applied Chemistry*, 3(5), 62-66.

Shah, M. K., & Maru, M. (2012). Transition metal complexes of 2-(substituted-lH-pyrozole-4-yl)-lH-benzo[d]imidazoles: Synthesis and characterization. *Journal of Chemical and Pharmaceutical Research*, 4(3), 1638-1643.

Stolle, A., Szuppa, T., Leonhardt, S. E. S., & Ondruschka, B. (2011). Ball milling in organic synthesis: Solutions and challenges. *Chemical Society Reviews*, 40(5), 2317-2329.

Suryanarayana, S. (2004). *Mechanical Alloying and Milling*. New York: Marcel Dekker.

Telia, A. C. (2011). Friendly synthesis of metal complexes of antimicrobial drugs. *Report from Center for Supramolecular Chemistry Research*, University of Cape Town, South Africa, 1-4.

Telia, A. C., Eke, U. B., & Owalude, S. O. (2013). Solvent-free mechanochemical synthesis and X-ray studies of Cu(II) and Ni(II) complexes of 5-(3,4,5-trimethoxybenzyl)pyrimidine-2,4-diamine (trimethoprim) in a ball-mill. *Journal of Saudi Chemical Society*, 17(1), 1319-6103.

Toussaint, K., Yang, X. C., Zielinski, M. A., Reigle, K. L., Sacavage, S. D., Nagar, S., & Raffa, R. B. (2010). What do we (not) know about how paracetamol works? *Journal of Clinical Pharmacy and Therapeutics*, 35(6), 617-638.

Tukur, D., Mishra, J., & Joshi, S. (2003). Synthesis and electrochemical study of analgesic drug acetaminophen. *International Journal of Advanced Engineering and Applied Sciences*, 3(4), 43-46.

Wang, G.-W. (2013). Mechanochemical organic synthesis. *Chemical Society Reviews*, 42(18), 7668-7700.

Wang, Z. L. (2000). Transition electron microscopy and spectroscopy of nanoparticles. In Z. L. Wang (Ed.), *Characterization of nanophase materials* (pp. 37-80). Weinheim: Wiley-VCH.

West, A. R. (2014). *Solid State Chemistry and its Application* (2nd ed.). New York: John Wiley & Sons.

Yousif, E., & Ahmed, A. (2013). Synthesis and characterization of transition metal complexes of 4-amino-5-pyridyl-4H-1,2,4-triazole-3-thiol. *Springer Open Journal*, 2(1), 510.

Yusha'u, M., & Salisu, F. U. (2011). Inhibition activity of Detarium microcarpum extract on some clinical bacterial isolates. *Biological and Environmental Science Journal for the Tropics*, 8(4), 113-117.